Effect of fragment emission time on the temperature of momentum quadrupole fluctuations

Fan Zhang,[1,2] Cheng Li,[1,2] Long Zhu,[1,2] Hang Liu,[3] and Feng-Shou Zhang[1,2,4,*]

[1]*The Key Laboratory of Beam Technology and Material Modification of Ministry of Education, College of Nuclear Science and Technology, Beijing Normal University, Beijing 100875, China*

[2]*Beijing Radiation Center, Beijing 100875, China*

[3]*Texas Advanced Computing Center University of Texas at Austin, Texas 78758, USA*

[4]*Center of Theoretical Nuclear Physics, National Laboratory of Heavy Ion Accelerator of Lanzhou, Lanzhou 730000, China*

(Received 22 December 2014; published 27 March 2015)

A systematic study of a momentum quadrupole fluctuation thermometer has been presented for heavy-ion collisions at 35 MeV/nucleon via the isospin-dependent quantum molecular dynamics model accompanied by the statistical decay model GEMINI. It is determined that the fragment momentum fluctuation temperature indeed reflects the average temperature of the excitation source in the fragmentation process and the secondary decay. We find that the divergence between the initial temperature and the final measurement temperature is different for protons, tritons, and ^{3}He. The maximum divergence of the temperature is about 20% probed by protons. As an example of using protons as the probe particle, we find that the isospin dependence of the nuclear temperature is consistent between the initial temperature and the final measurement temperature.

DOI: 10.1103/PhysRevC.91.034617 PACS number(s): 25.70.Mn, 25.70.Pq, 24.60.−k

I. INTRODUCTION

The concept of a nuclear temperature, which comes from the definition of the compound nucleus, was introduced some 70 years ago [1–3]. Temperature is a very important thermodynamic quantity in the nuclear equation of state (EOS) which is of broad interest for its importance in nucleosynthesis, heavy-ion collisions, supernovae dynamics, and neutron stars [4–7]. To examine the EOS, the relation between thermodynamic quantities is studied. These could be, for example, pressure and temperature, density and temperature, or temperature and energy; this last is commonly referred to as the caloric curve and has been measured for many finite nuclear systems. Therefore, a precise determination of the temperature achieved in nuclear reactions has become a priority in the study of heavy-ion reactions.

For many years, various thermometers have been used to expand the experimental understanding of nuclear systems. These studies have often been motivated by the desire to define the proposed nuclear liquid-gas phase transition [8–10]. A broad array of caloric curves have been obtained allowing a better understanding of the nuclear limiting temperature and its dependence on source excitation energy as well as source size [11]. Recently, the asymmetry dependence of the nuclear caloric curve was studied using a momentum quadrupole fluctuation (MQF) thermometer [12,13]. Additionally, nuclear thermometry has provided a bridging connection between isoscaling [14–16] and the symmetry coefficient of the nuclear equation of state [17,18].

In many studies, the nuclear temperature has been obtained from energy spectra through moving source fitting [19–21]. However, this thermometer is known to exhibit nonthermal and collective behavior [22]. Alternatively, temperature may be obtained through isotopic thermometers. The double isotope thermometer has provided much data [23–25]; however, the temperatures derived are complicated by model-dependent secondary decay corrections [25–27].

Recently, another thermometer based on fragment momentum fluctuations was presented by Wuenschel *et al.* [28]. The MQF thermometer has been used to estimate the temperature of the quasiprojectile (QP) sources. However, the kinematic characteristics of fragments reflect not only the thermal properties of the system, but also the Fermi motion at freeze-out, recoil effects, radial flow effects, and emission time effects. If we want to extract the thermal temperature from kinematic distributions, we must analyze the above effects in detail. Using the methods suggested by Bauer [22] and Zheng *et al.* [29], one can eliminate the influence of the Fermi motion and extract the temperatures from kinematic distributions of fragments. Coulomb corrections to the extraction of the temperature have also been studied [30,31]. However, there are few studies of the fragment emission time effects on the MQF thermometer for different particles and neutron-proton asymmetry.

II. MODEL AND METHOD

In the present work, we study the MQF thermometer within the framework of the isospin-dependent quantum molecular dynamics (IQMD) model [32–35] incorporating the statistical decay model GEMINI [36]. In the IQMD model, the Hamiltonian H is expressed as

$$H = T + U_{\text{Coul}} + \int V(\rho) d\mathbf{r}, \quad (1)$$

where T is the kinetic energy and U_{Coul} is the Coulomb potential energy. $V(\rho)$ is the nuclear potential energy density functional, which is written as

$$V(\rho) = \frac{\alpha}{2}\frac{\rho^2}{\rho_0} + \frac{\beta}{\gamma+1}\frac{\rho^{\gamma+1}}{\rho_0^{\gamma}} + \frac{g_{\text{sur}}}{2}\frac{(\nabla\rho)^2}{\rho_0} + V_{\text{sym}}. \quad (2)$$

$$V_{\text{sym}} = \frac{C_{\text{sym}}}{2}\frac{(\rho_n - \rho_p)^2}{\rho_0}. \quad (3)$$

*Corresponding author: fszhang@bnu.edu.cn

The parameters α, β, and γ are taken as -356 MeV, 303 MeV, and 1.17, respectively, and the corresponding compressibility is 200 MeV [37]. $C_{\rm sym} = 39.4$ MeV is the symmetry energy strength. $g_{\rm sur}$ is taken as 130 MeV fm^5. The first and the second terms in Eq. (2) are the two-body and three-body terms, respectively. The third one is the surface term and the last one corresponds to the symmetry energy. The binary nucleon-nucleon collisions are included. The binary collisions are allowed if two requirements are satisfied. First, the nucleons must pass the point of closest approach within the interval. Second, the distance of closest approach must be less than $b_{\rm max} = \sqrt{\sigma_{nn}/\pi}$. Here σ_{nn} is the nucleon-nucleon collision cross section. In addition, Pauli blocking (of the final state) is taken into account. For each collision the phase-space occupation f_i is calculated by performing the integration on a hypercube of volume h^3 in the phase space centered around the final states [38]. The collision is accepted if the phase-space occupations f_i at the final state are both less than 1. The phase-space density constraint on the time evolution of the momentum space distribution is also taken into account.

The QP sources are produced in the reactions of ^{70}Zn + ^{70}Zn, ^{64}Zn + ^{64}Zn, and ^{64}Ni + ^{64}Ni at $E/A = 35$ MeV. To examine the divergence of the MQF temperature $T_{\rm MQF}$ between the initial temperature and the final measurement temperature, it is desired to select equilibrated QP sources. Three cuts are made on the particle and event characteristics. To exclude fragments that clearly do not originate from a QP, the fragment velocity in the beam direction v_z is restricted relative to the velocity of the largest fragment measured in the event $v_{z,\rm res}$. (i) The accepted window on $\frac{V_z}{V_{z,\rm res}}$ is 1 ± 0.65 for $Z = 1$, 1 ± 0.6 for $Z = 2$, and 1 ± 0.45 for $Z \geqslant 3$. (ii) The mass of the reconstructed QP is required to be $48 \leqslant A \leqslant 52$, satisfying the requirements. (iii) To further select the equilibrated QP, spherical QPs are selected by a constraint on the longitudinal momentum p_z and transverse momentum p_t of the fragments comprising the QP: $-0.3 \leqslant \log_{10}(Q_{\rm shape}) \leqslant 0.3$, where $Q_{\rm shape} = \frac{\sum p_z^2}{\sum \frac{1}{2} p_t^2}$ with the sums extending over all fragments of the QP. For more details, see Ref. [12].

We need to mention that we use different methods to calculate the multiplicity of neutrons. Using a molecular dynamics model, the free neutrons can be found in phase space. The average kinetic energy per free neutron ascribed to the QP is given by $2.2 + 1.25(E_{\rm cp}/A_{\rm cp})$ MeV/nucleon [12], where $E_{\rm cp}$ is the total energy of the charged particles in the transverse direction and $A_{\rm cp}$ is the mass of the QP calculated using only charged particles. Because the QP is in equilibrium, the free neutrons emitting can be seen isotropically in the center-of-mass frame of the fragmenting source. Using the average kinetic energy, we can calculate the neutron's maximum velocity $V_n^{\rm max}$ and minimum velocity $V_n^{\rm min}$ in the beam direction. Therefore, we can estimate the multiplicity of neutrons by the accepted window on $V_n^{\rm min} \leqslant V_n \leqslant V_n^{\rm max}$.

The momentum quadrupole is defined as

$$Q_{xy} = p_x^2 - p_y^2, \tag{4}$$

using the transverse components p_x and p_y of the particle's momentum in the frame of the QP source. If the approximation is made that the emitted particles are described by a Maxwell-Boltzmann distribution, the variance of Q_{xy} is related to the temperature by

$$\langle \sigma_{xy}^2 \rangle = 4m^2T^2, \tag{5}$$

where m is the probe particle mass [28].

To identify the emitted particles at the time the particles were produced, the nuclear fragments are constructed by using the coalescence model, in which nucleons with relative momentum smaller than 300 MeV/c and relative distance smaller than 3.5 fm will be combined into a cluster. The simulation time in this work is 800 fm/c, which allows the QP having enough time to fragment.

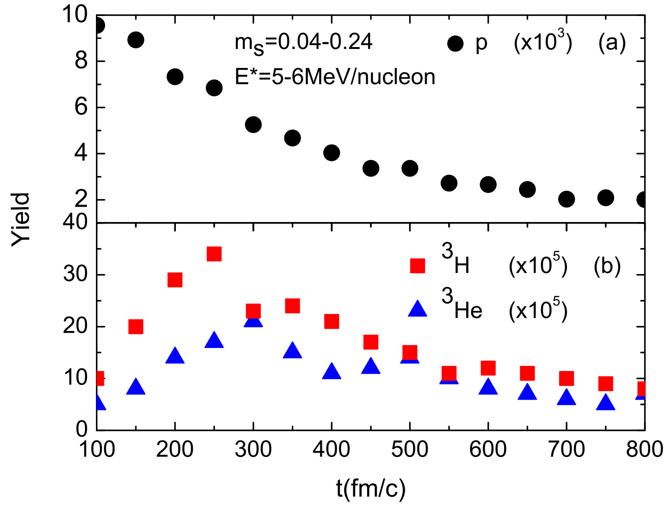

FIG. 1. (Color online) Time evolution of yields obtained from the sources with mass $48 \leqslant A \leqslant 52$ and all asymmetries.

III. RESULTS AND DISCUSSION

Figure 1 shows the time evolution of the protons yields, tritons yields, ^{3}He yields (those produced in intervals of 50 fm/c), in the frame of the fragmenting QP source at excitation energy per nucleon 5–6 MeV/nucleon. We can see that the proton yields decrease quickly during the period of maximum evaporation (i.e., from 100 to 500 fm/c). After 500 fm/c, the protons production are almost constant, which is about 0.002. The production of tritons and ^{3}He has two distinct regions: an increase stage and a decrease stage. Several observations are immediate. Most tritons and ^{3}He are produced during the period of maximum evaporation, but there is some production after 500 fm/c. Thus, as the QP deexcites, each particle emission changes its composition slightly. Using the temperature probed by the emitted particles, which are emitted over a range of times, could mask the true information of the QP. The time of the earliest emission particles from the QP is about 100 fm/c. Thus, in this paper, we define 100 fm/c as the time of the QP formation, the temperature calculated by emission particles before 150 fm/c as the "initial" temperature T_i, and 800 fm/c as the final measurement temperature T_f.

To further investigate the particle emission time effects on the $T_{\rm MQF}$ for different temperatures and particles, we display the $T_{\rm MQF}$ that were derived from protons, tritons,

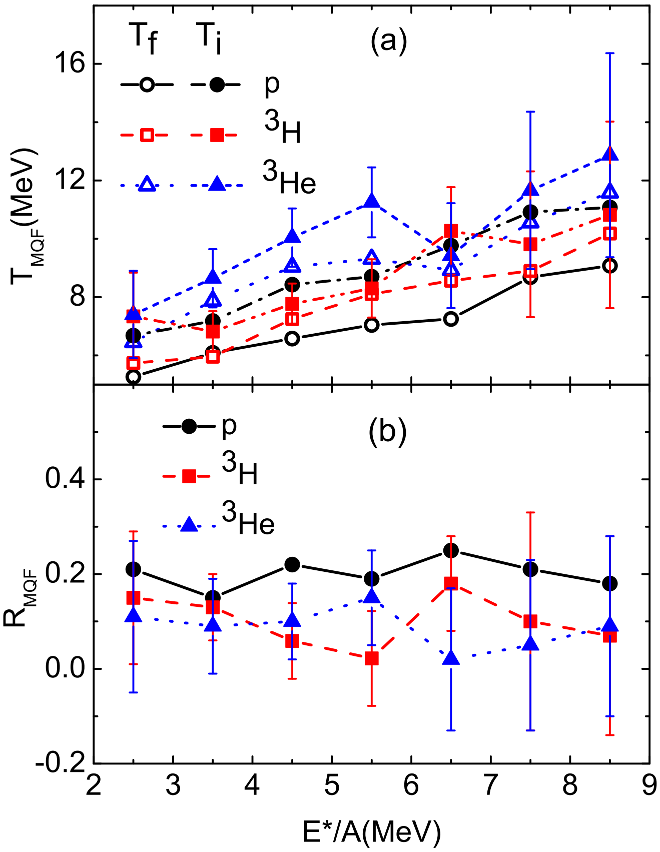

FIG. 2. (Color online) (a) Momentum quadrupole fluctuation temperatures for initial temperature (full shape) and final measurement temperature (open shape) extracted with light charged particle probes. (b) R_{MQF} versus excitation energy per nucleon.

and ^{3}He emissions for sources with mass $48 \leqslant A \leqslant 52$ and all asymmetries in Fig. 2. The asymmetry of the source is defined as

$$m_s = \frac{N_s - Z_s}{A_s}, \tag{6}$$

where N_s, Z_s, and A_s are the neutron number, proton number, and mass number. Temperatures are calculated for 1-MeV-wide bins in excitation energy per nucleon. It can be seen from Fig. 2(a) that the T_i of the QP is greater than the T_f probed by the emitted particles, which are emitted over a range of times. Recently, Zheng *et al.* [39] also studied the deexcitation of an excited nucleus using the GEMINI model which assumes a sequential decay of an excited nucleus. They found that the momentum fluctuation temperature shifts down due to the sequential decay. Our result is consistent with theirs. However, in our calculations the GEMINI model is only applied to simulate the decay of prefragments. Most of the excitation energy of the QP is released in the fragmentation process, which is simulated by the IQMD model.

For ^{3}He, the divergence of the temperature between T_i and T_f is smaller than for protons. The difference in the T_i for protons, tritons, and ^{3}He still exists. It is possible that some of the difference is the result of Coulomb contribution and Fermi momentum in the detected fragments. The particle emission

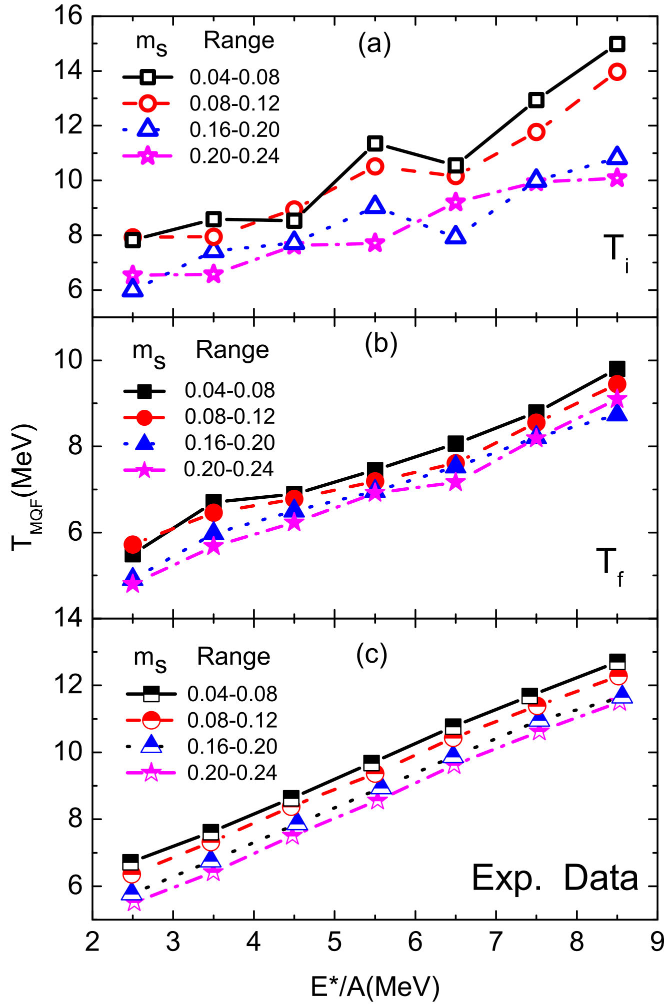

FIG. 3. (Color online) Caloric curves for protons, selected on source asymmetry. The different curves correspond to narrow selections on the source asymmetry for the (a) initial temperature, (b) final measurement temperature, and (c) experimental data [12].

time effects on the T_{MQF} can be seen more clearly from the ratio R_{MQF} versus excitation energy per nucleon E^*/A, which is shown in Fig. 2(b). The R_{MQF} can be obtained from the T_i and T_f through

$$R_{\mathrm{MQF}} = (T_i - T_f)/T_i. \tag{7}$$

Significant particle emission time effects at constant excitation energy may be seen in the T_i and T_f. For protons, the R_{MQF} is about 0.2 across all E^*/A. Thus, using the T_f as the temperature of the QP may mask the real nature of the QP. It is worth noting that proton, triton, and ^{3}He yields are all impacted by emission time. However, there are little effects on tritons and ^{3}He. This result may be attributable to the energy cost for their emission from an excited source. Some ^{3}He and tritons are emitted at a later stage, but the excitation energy of excited source is still high. For protons the cost energy for their emission is low relative to ^{3}He and tritons. Therefore, protons are more easily impacted by emission time.

Figure 3 shows T_{MQF} as a function of excitation energy per nucleon of the QP, as determined with the MQF thermometer

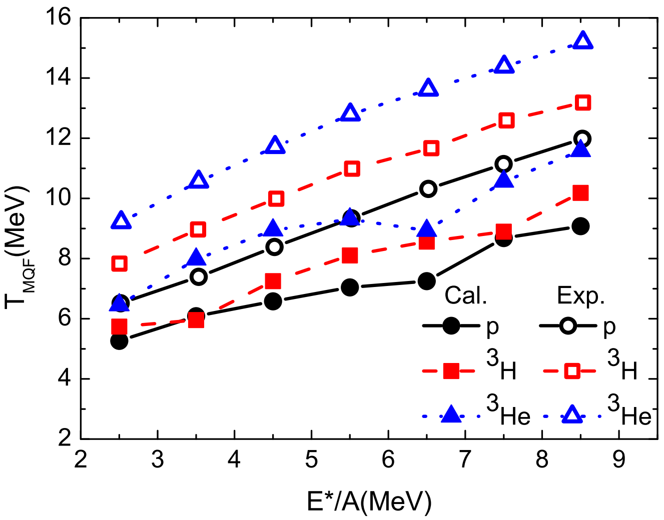

FIG. 4. (Color online) Momentum quadrupole fluctuation temperatures for sources with mass $48 \leqslant A \leqslant 52$ and all asymmetries, extracted with light charged particle probes. Experimental data are taken from McIntosh *et al.* [12].

using protons as the probe particle. To examine in more detail the temperature shift of the emission time with the changing source asymmetry, we plot caloric curves for different time ranges in Fig. 3. In Fig. 3(a), the caloric curves were obtained with the MQF thermometer using early emitted protons. It is clear that the temperature of the neutron-poor QP is higher. In Fig. 3(b), the caloric curves are obtained using the emitted protons, which are emitted over a range of times. We can see that the isospin dependence of the nuclear temperature is consistent between the T_i and T_f.

It can be seen from Figs. 3(b) and 3(c) that the T_f by the model follows the trend of the experimental data. Each curve corresponds to a narrow selection in the asymmetry of the QP source. It is worth noting that Su *et al.* [33] also studied the asymmetry dependence of the temperature through isotopic yield ratios by using the IQMD model. However, the result is just the reverse. They found that the temperatures for the neutron-rich projectiles are larger than those for the neutron-poor projectiles. The origin of this difference may be in the choosing of the source or the different nature of the two thermometers.

Figure 4 shows the T_f of the QP, as a function of the excitation energy per nucleon E^*/A of the QP, measured with the MQF thermometer using protons, tritons, and ^{3}He as probe particles. For a given excitation energy per nucleon, the protons show the lowest temperature, followed by the trions and ^{3}He. The ordering of the temperature for the different light charged particle (LCP) species is consistent with the data [12].

IV. CONCLUSION

In conclusion, we performed a study of the momentum quadrupole fluctuation temperature T_{MQF} achieved in heavy-ion reactions. An isospin-dependent quantum molecular dynamics (IQMD) model incorporating the statistical decay model GEMINI was used for a variety of reactions to extract the temperature T_{MQF}. The divergence of the temperature T_{MQF} between the initial temperature T_i and the final measured temperature T_f was obtained using the instantaneous and cumulative yields of the protons, tritons, and ^{3}He. Our results can be summarized as follows: (i) The divergence of the T_{MQF} between the T_f and T_i is about 20% for proton, 12% for tritons, and 10% for ^{3}He. Using the temperature probed by the emission particles, which are emitted over a range of times, may mask the true nature of the QP. (ii) The isospin dependence of the nuclear temperature is consistent between the T_i and T_f using protons as the probe particle. (iii) The ordering of the temperature for the different light charged particles by the model follows the trend of the experimental data.

ACKNOWLEDGMENTS

This work was supported by the National Natural Science Foundation of China under Grants No. 11025524 and No.11161130520 and the National Basic Research Program of China under Grant No. 2010CB832903, the European Commission's 7th Framework Programme (Fp7-PEOPLE-2010-IRSES) under Grant Agreement Project No. 269131.

[1] N. Bohr, Nature **137**, 344 (1936).
[2] V. F. Weisskopf, Phys. Rev. **52**, 295 (1937).
[3] H. A. Bethe, Rev. Mod. Phys. **9**, 69 (1937).
[4] H. T. Janka, K. Langanke, A. Marek, G. Martinez-pinedo, and B. Müller, Phys. Rep. **442**, 38 (2007).
[5] P. Danielewicz, R. Lacey, and W. G. Lynch, Science **298**, 1592 (2002).
[6] B. A. Li, L. W. Chen, and C. M. Ko, Phys. Rep. **464**, 113 (2008).
[7] J. M. Lattimer and M. Parkash, Science **304**, 536 (2004).
[8] A. Kelić, J. B. Natowitz, and K.-H. Schmidt, Eur. Phys. J. A **203**, 30 (2006).
[9] B. Borderie and M. F. Rivet, Prog. Part. Nucl. Phys. **551**, 61 (2008).
[10] A. Bonasera, Z. Chen, R. Wada, K. Hagel, J. Natowitz, P. Sahu, L. Qin, S. Kowalski, T. Keutgen, T. Materna, and T. Nakagawa, Phys. Rev. Lett. **101**, 122702 (2008).
[11] J. B. Natowitz, R. Wada, K. Hagel, T. Keutgen, M. Murray, A. Makeev, L. Qin, P. Smith, and C. Hamilton, Phys. Rev. C **65**, 034618 (2002).
[12] A. B. McIntosh, A. Bonasera, Z. Kohley, P. J. Cammarata, K. Hagel, L. Heilborn, J. Mabiala, L. W. May, P. Marini, A. Raphelt, G. A. Souliotis, S. Wuenschel, A. Zarrella, and S. J. Yennello, Phys. Rev. C **87**, 034617 (2013).
[13] A. B. McIntosh, A. Bonasera, P. Cammarata, K. Hagel, L. Heilborn, Z. Kohley, J. Mabiala, L. W. May, P. Marini, A. Raphelt, G. A. Soulitois, S. Wuenschel, A. Zarrella, and S. J. Yennello, Phys. Lett. B **719**, 337 (2013).
[14] M. B. Tsang, C. K. Gelbke, X. D. Liu, W. G. Lynch, W. P. Tan, G. Verde, H. S. Xu, W. A. Friedman, R. Donangelo, S. R. Souza, C. B. Das, S. DasGupta, and D. Zhabinsky, Phys. Rev. C **64**, 054615 (2001).

[15] M. B. Tsang, W. A. Friedman, C. K. Gelbke, W. G. Lynch, G. Verde, and H. S. Xu, Phys. Rev. Lett. **86**, 5023 (2001).
[16] H. S. Xu, M. B. Tsang, T. X. Liu, X. D. Liu, W. G. Lynch, W. P. Tan, A. Vander Molen, G. Verde, A. Wagner, H. F. Xi, C. K. Gelbke, L. Beaulieu, B. Davin, Y. Larochelle, T. Lefort, R. T. deSouza, R. Yanez, V. E. Viola, R. J. Charity, and L. G. Sobotka, Phys. Rev. Lett. **85**, 716 (2000).
[17] A. Le Fèvre, G. Auger, M. L. Begemann-Blaich, N. Bellaize, R. Bittiger, F. Bocage, B. Borderie, R. Bougault, B. Bouriquet, J. L. Charvet, A. Chbihi, R. Dayras, D. Durand, J. D. Frankland, E. Galichet, D. Gourio, D. Guinet, S. Hudan, G. Immé, P. Lautesse, F. Lavaud, R. Legrain, O. Lopez, J. Łukasik, U. Lynen, W. F. J. Müller, L. Nalpas, H. Orth, E. Plagnol, G. Raciti, E. Rosato, A. Saija, C. Schwarz, W. Seidel, C. Sfienti, B. Tamain, W. Trautmann, A. Trzciński, K. Turzó, E. Vient, M. Vigilante, C. Volant, B. Zwiegliński, and A. S. Botvina, Phys. Rev. Lett. **94**, 162701 (2005).
[18] D. V. Shetty, S. J. Yennello, and G. A. Souliotis, Phys. Rev. C **76**, 024606 (2007).
[19] R. Wada, D. Fabris, K. Hagel, G. Nebbia, Y. Lou, M. Gonin, J. B. Natowitz, R. Billerey, B. Cheynis, A. Demeyer, D. Drain, D. Guinet, C. Pastor, L. Vagneron, K. Zaid, J. Alarja, A. Giorni, D. Heuer, C. Morand, B. Viano, C. Mazur, C. Ngo, S. Leray, R. Lucas, M. Ribrag, and E. Tomasi, Phys. Rev. C **39**, 497 (1989).
[20] A. S. Hirsch, A. Bujak, J. E. Finn, L. J. Gutay, R. W. Minich, N. T. Porile, R. P. Scharenberg, B. C. Stringfellow, and F. Turkot, Phys. Rev. C **29**, 508 (1984).
[21] T. Odeh, R. Bassini, M. Begemann-Blaich, S. Fritz, S. J. Gaff-Ejakov, D. Gourio, C. Groß, G. Immé, I. Iori, U. Kleinevoß, G. J. Kunde, W. D. Kunze, U. Lynen, V. Maddalena, M. Mahi, T. Möhlenkamp, A. Moroni, W. F. J. Müller, C. Nociforo, B. Ocker, F. Petruzzelli, J. Pochodzalla, G. Raciti, G. Riccobene, F. P. Romano, A. Saija, M. Schnittker, A. Schüttauf, C. Schwarz, W. Seidel, V. Serfling, C. Sfienti, W. Trautmann, A. Trzcinski, G. Verde, A. Wörner, Hongfei Xi, and B. Zwieglinski, Phys. Rev. Lett. **84**, 4557 (2000).
[22] W. Bauer, Phys. Rev. C **51**, 803 (1995).
[23] M. B. Tsang, W. G. Lynch, H. Xi, and W. A. Friedman, Phys. Rev. Lett. **78**, 3836 (1997).
[24] W. C. Hsi, G. J. Kunde, J. Pochodzalla, W. G. Lynch, M. B. Tsang, M. L. Begemann-Blaich, D. R. Bowman, R. J. Charity, F. Cosmo, A. Ferrero, C. K. Gelbke, T. Glasmacher, T. Hofmann, G. Imme, I. Iori, J. Hubele, J. Kempter, P. Kreutz, W. D. Kunze, V. Lindenstruth, M. A. Lisa, U. Lynen, M. Mang, A. Moroni, W. F. J. Müller, M. Neumann, B. Ocker, C. A. Ogilvie, G. F. Peaslee, G. Raciti, F. Rosenberger, H. Sann, R. Scardaoni, A. Schüttauf, C. Schwarz, W. Seidel, V. Serfling, L. G. Sobotka, L. Stuttge, S. Tomasevic, W. Trautmann, A. Tucholski, C. Williams, A. Wörner, and B. Zwieglinski, Phys. Rev. Lett. **73**, 3367 (1994).
[25] W. Trautmann, R. Bassini, M. Begemann-Blaich, A. Ferrero, S. Fritz, S. J. Gaff-Ejakov, C. Groß, G. Imme, I. Iori, U. Kleinevoß, G. J. Kunde, W. D. Kunze, A. Le Fèvre, V. Lindenstruth, J. Łukasik, U. Lynen, V. Maddalena, M. Mahi, T. Möhlenkamp, A. Moroni, W. F. J. Müller, C. Nociforo, B. Ocker, T. Odeh, H. Orth, F. Petruzzelli, J. Pochodzalla, G. Raciti, G. Riccobene, F. P. Romano, Th. Rubehn, A. Saija, H. Sann, M. Schnittker, A. Schüttauf, C. Schwarz, W. Seidel, V. Serfling, C. Sfienti, A. Trzciński, A. Tucholski, G. Verde, A. Wörner, Hongfei Xi, and B. Zwiegliński, Phys. Rev. C **76**, 064606 (2007).
[26] V. E. Viola and R. Bougault, Eur. Phys. J. A **30**, 215 (2006).
[27] R. Wada, R. Tezkratt, K. Hagel, F. Haddad, A. Kolomiets, Y. Lou, J. Li, M. Shimooka, S. Shlomo, D. Utley, B. Xiao, N. Mdeiwayeh, J. B. Natowitz, Z. Majka, J. Cibor, T. Kozik, and Z. Sosin, Phys. Rev. C **55**, 227 (1997).
[28] S. Wuenschel, A. Bonasera, L. W. May, G. A. Souliotis, R. Tripathi, S. Galanopoulos, Z. Kohley, K. Hagel, D. V. Shetty, K. Huseman, S. N. Soisson, B. C. Stein, and S. J. Yennello, Nucl. Phys. A **843**, 1 (2010).
[29] H. Zheng and A. Bonasera, Phys. Lett. B **696**, 178 (2011).
[30] H. Zheng, G. Giuliani, and A. Bonasera, Phys. Rev. C **88**, 024607 (2013).
[31] H. Zheng, G. Giuliani, and A. Bonasera, J. Phys. G: Nucl. Part. Phys. **41**, 055109 (2014).
[32] C. Hartnack, Li. Zhuxia, L. Neise, G. Peilert, A. Rosenhauer, H. Sorge, J. Aichelin, H. Stöcker, and W. Greiner, Nucl. Phys. A **495**, 303 (1989).
[33] J. Su and F. S. Zhang, Phys. Rev. C **84**, 037601 (2011).
[34] C. Liewen, Z. Fengshou, and J. Genming, Phys. Rev. C **58**, 2283 (1998).
[35] L. W. Chen, F. S. Zhang, G. M. Jin, and Z. Y. Zhu, Phys. Lett. B **459**, 21 (1999).
[36] R. J. Charity, M. A. McMahan, G. J. Wozniak, R. J. McDonald, L. G. Moretto, D. G. Sarantites, L. G. Sobotka, G. Guarino, A. Pantaleo, L. Fiore, A. Gobbi, and K. D. Hildenbrand, Nucl. Phys. A **483**, 371 (1988).
[37] J. Aichelin, Phys. Rep. **202**, 233 (1991).
[38] M. Papa, T. Maruyama, and A. Bonasera, Phys. Rev. C **64**, 024612 (2001).
[39] H. Zheng, G. Bonasera, J. Mabiala, P. Marini, and A. Bonasera, Eur. Phys. J. A **50**, 167 (2014).